^{19}F NMR Chemical Shifts. 1. Aliphatic Fluorides

Kenneth B. Wiberg* and Kurt W. Zilm*

Department of Chemistry, Yale University, New Haven Connecticut 06520-8107

kenneth.wiberg@yale.edu

Received December 11, 2000

The ^{19}F NMR shielding for the alkyl fluorides from methyl fluoride to *tert*-butyl fluoride has been calculated using IGAIM and has been separated into the contribution from each of the molecular orbitals. The relatively large change in fluorine shielding, in contrast to the adjacent carbon, was found to be due to the tensor components normal to the C−F bond axis. As the number of adjacent p-orbitals increases, the lone-pair p orbitals at fluorine become involved with MOs using these orbitals. The increase in the number of occupied orbitals associated with the fluorine leads to increased opportunities for mixing with virtual orbitals and to the increase in paramagnetic deshielding. The same pattern is seen on going from acetylene to 2-*tert*-butylacetylene and is also seen in the methyl ^{13}C shielding in the series ethane, propane, isobutane, and neopentane. The fluorine shielding in the series of fluoromethanes also decreases with increasing fluorine substitution. With carbon tetrafluoride, the decreased shielding arises from the highest occupied MO, which is a nonbonding linear combination of pure p functions at the fluorines.

1. Introduction

^{19}F NMR chemical shifts have received much attention, and experimental isotropic shifts are available for a wide variety of structural types.[1] These shifts have been correlated with inductive and resonance parameters, electron densities, and other properties.[1,2] It has been found that ab initio calculations of ^{19}F shielding reproduce the experimental shielding for fluoroalkanes[3] and for fluorobenzenes.[4] The ^{19}F NMR shielding effects in some cyclic and bicyclic fluorides have been examined and have been correlated with the results of the natural bond orbital approach.[5]

Despite these studies, there are many aspects of ^{19}F chemical shifts that are not well understood. Table 1 summarizes the available data[1] for a series of simple fluorides. Here, the data are presented as shielding (σ_F) with respect to a bare fluorine nucleus. Using the chemical shift (δ_F) convention that increasing shielding (upfield shift) is signified by larger negative values, the two are related by

$$\sigma_F = 188.7 - \delta_F$$

where 188.7 is the shielding of $FCCl_3$,[6] the commonly used reference for ^{19}F chemical shifts. Shielding is the quantity that is calculated via theoretical methods, and it has more physical significance than the chemical shift. Similarly, the shielding (σ_C) and chemical shift (δ_C) for carbon are related by

$$\sigma_C = 186.4 - \delta_C$$

where 186.4 is the shielding of the commonly used reference tetramethylsilane.[7]

Table 1. Calculated and Observed Isotropic Shielding for Carbon and Fluorine, ppm

	CH_3			C(F)			F		
compd	GIAO	IGAIM	obsd	GIAO	IGAIM	obsd	GIAO	IGAIM	obsd[1]
CH_3F	113	113	115	468	468	461			
CH_3CH_2F	168	169	171	103	104	106	409	410	402
$(CH_3)_2CHF$	162	163	164	96	96	99	363	363	353
$(CH_3)_3CF$	157	157	158	90	90	93	332	332	321
CH_2CF_2				72	72	77	332	332	332
CHF_3				61	61	68	264	265	269
CF_4				55	54	64	245	245	250
CH_3Cl				155	157	161	925	934	
CH_3CH_2Cl	166	166	168	138	140	147	819	831	
$(CH_3)_2CHCl$	157	158	159	124	125	133	726	740	
$(CH_3)_3CCl$	150	151	152	111	111	120	655	666	

Table 2. Calculated Energies and Structures

	B3P86			
compd	6-311G*	6-311+G(3df,2p)	*r*(CF) Å	*r*(CC) Å
CH_3F	−140.09508	−140.11499	1.379	
CH_3CH_2F	−179.57136	−179.59467	1.390	1.506
$(CH_3)_2CHF$	−219.04656	−219.07424	1.402	1.510
$(CH_3)_3CF$	−258.52011	−258.55253	1.413	1.517
CH_2F_2	−239.50531	−239.53273	1.354	
CHF_3	−338.92697	−338.96073	1.334	
CF_4	−438.34853	−438.38461	1.321	

An examination of Table 1 shows that the solution-phase isotropic shielding of fluorine decreases markedly on going from methyl to ethyl, isopropyl, and *tert*-butyl as substituents. At the same time, the shielding of the carbon to which the fluorine is bonded also decreases, but by a smaller amount.

(1) Emsley, J. W.; Feeney, J.; Sutcliffe, L. H. *Prog. NMR Spectrosc* **1971**, *7*, 1.
(2) For a recent review on NMR shielding theory, see: Jameson, C. J. *ACS Symp. Ser.* **1999**, *732* (Modeling NMR Chemical Shifts) 1.
(3) Tanuma, T.; Irisawa, J.; Ohnishi, K. *J. Fluorine Chem.* **2000**, *102*, 205. Tanuma, T.; Irisawa, J. *J. Fluorine Chem.* **1999**, *99*, 157.
(4) Karadakov, P. B.; Webb, G. A.; England, J. A. *ACS Symp. Ser.* **1999**, *732* (Modeling NMR Chemical Shifts), 115.
(5) Adcock, W.; Lunsmann, D.; Peralta, J. E.; Contreras, R. H. *Magn. Reson. Chem.* **1999**, *37*, 167.
(6) Jameson, C. J.; Jameson, A. K.; Burrell, P. M. *J. Chem. Phys.* **1980**, *73*, 6013.
(7) Jameson, A. K.; Jameson, C. J. *Chem. Phys. Lett.* **1987**, *134*, 461. Raynes, W. T.; McVay, R.; Wright, S. *J. Chem. Soc., Faraday Trans. 2* **1989**, *85*, 759.

10.1021/jo001726g CCC: $20.00
Published on Web 03/29/2001

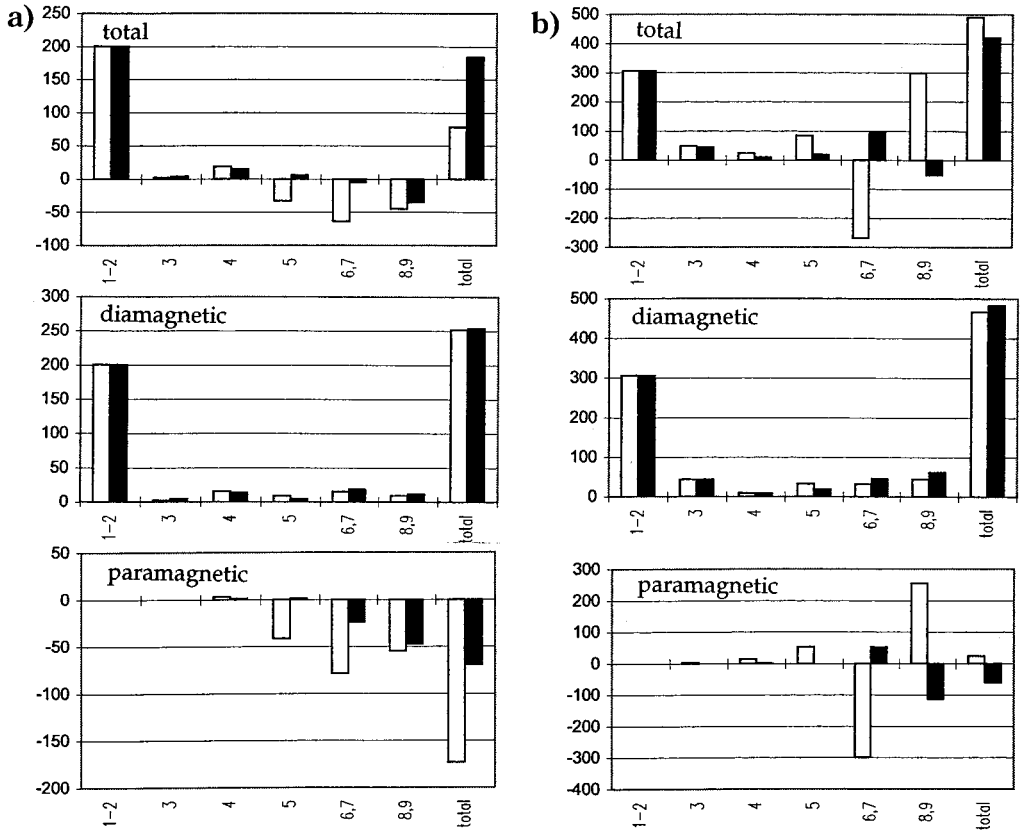

Figure 1. Magnetic shielding for methyl fluoride on an MO basis. (a) Carbon: the upper plot gives the total shielding, the center plot gives the diamagnetic shielding, and the lower plot gives the paramagnetic shielding. (b) Fluorine: the ⊥ components are indicated by open bars, and the || components are indicated by solid bars.

Table 3. Effect of H−C−F Bond Angle on the Shielding of Methyl Fluoride B3P86/6-311G* Optimizations, B3P86/6-311+G(3df,2p) Calculations

∠HCF (deg)	*r*(CF) Å	*r*(CH) Å	σ_C (ppm)	σ_F (ppm)
110.0	1.3746	1.0929	113.7	469.5
109.14[a]	1.3787	1.0924	112.8	468.5
108.0	1.3837	1.0917	111.8	467.5
106.0	1.3937	1.0905	110.0	466.0
104.0	1.4048	1.0894	108.3	464.8
102.0	1.4171	1.0883	106.7	464.1

[a] Optimized bond angle.

One might expect alkyl groups and fluorines to have opposite effects as substituents since the former are electron releasing and the latter are electron withdrawing. However, in the series methyl fluoride, methylene fluoride, fluoroform, and carbon tetrafluoride, the same trend is seen. Increasing fluorine substitution leads to decreased shielding of both the carbons and the fluorines.

We shall try to develop an understanding of these shielding changes based on molecular orbital calculations, including a breakdown of the MO contributions to the shielding.[8]

2. Calculations

The structures of the compounds were obtained from B3P86/6-311G* geometry optimizations. The shielding was calculated using both GIAO[9] and IGAIM[10] with the B3P86/6-311+G(3df,2p) theoretical model. The B3P86 density functional[11] was chosen since we have found it to be one of the more successful functionals for reproducing both NMR chemical shifts[12] and the energies of electronically excited states.[13] The basis set has been found to be generally successful in NMR shielding calculations.[9c] The calculations were carried out using Gaussian-99.[14]

Table 4. Tensor Components for the Fluorines of Fluoroalkanes, ppm

compd	σ_x	σ_y	σ_z
CH_3F	490	490	424
CH_3CH_2F	451	392	385
$(CH_3)_2CHF$	360	336	386
$(CH_3)_3CF$	310	310	375

GIAO is the more familiar method for calculating shielding, where the latter is obtained as the second derivative of the energy with respect to the applied field and the nuclear moment using orbitals that are modified to make the calculation field independent. In the IGAIM method, the current density is first calculated using conventional orbitals. The shielding density about a given atom is obtained as the cross product of the current density and a vector from the nucleus to the given point, divided by the distance cubed. The shielding is obtained by integrating the shielding density. The current density may be calculated on an MO basis, and the paramagnetic and diamagnetic terms may be obtained separately.[8] This

(8) Wiberg, K. B.; Hammer, J. D.; Zilm, K. W.; Cheeseman, J. R.; Keith, T. A. *J. Phys. Chem. A* **1998**, *102*, 8766.

(9) (a) Ditchfield, R. *Mol. Phys.* **1974**, *27*, 789. (b) Wolinski, K.; Hinton, J. F.; Pulay, P. *J. Am. Chem. Soc.* **1990**, *112*, 8251. (c) For the implementation that is found in Gaussian-95, see: Cheeseman, J. R.; Trucks, G. W.; Keith, T. A.; Frisch, M. J. *J. Chem. Phys.* **1996**, *104*, 5497.

(10) Keith, T. A.; Bader, R. F. W. *Chem. Phys. Lett.* **1993**, *210*, 223.

(11) Adamo, C.; Barone, V. *Chem. Phys. Lett.* **1997**, *274*, 242. Perdew, J. P.; Burke, K.; Wang, Y. *Phys. Rev.* **1996**, *B54*, 16533

(12) Wiberg, K. B. *J. Comput. Chem.* **1999**, *20*, 1299.

(13) Wiberg, K. B.; Stratmann, E.; Frisch, M. J. *Chem. Phys. Lett.* **1998**, *297*, 60.

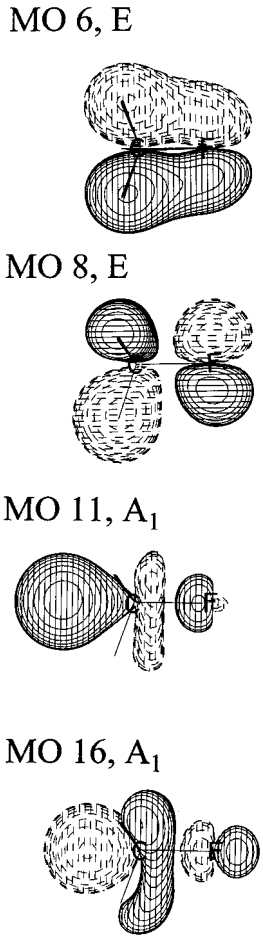

Figure 2. Molecular orbitals of methyl fluoride. MO 6 and 8 are occupied, MO 11 and 16 are virtual orbitals.

allows the shielding to be obtained in the same fashion. The diamagnetic part is concerned only with the ground-state electron density distribution, whereas the paramagnetic part is derived from the interaction of filled MOs with vacant MOs in the presence of a magnetic field. The GIAO and IGAIM methods lead to essentially the same (~±2 ppm) calculated shielding with the B3P86/6-311+G(3df,2p) basis set.

It is helpful to have a reference for the maximum diamagnetic shielding for both ^{19}F and ^{13}C. Fluoride ion, having spherical symmetry, can only have diamagnetic shielding, and the calculations give a value of 480 ppm. This is partitioned in the following fashion: 1s, 306; 2s, 50.3; 2p (six electrons) 123.6 ppm. Similarly, C^{4-} should give close to the maximum diamagnetic shielding for carbon, and the calculations give a value of 285 ppm. This is partitioned as follows: 1s, 200.7; 2s, 24.7; 2p, 57.3 ppm. The magnitude of the shielding depends on the distance from the nucleus; thus, $\sigma_F(1s) > \sigma_F(2s)$. The higher nuclear charge of fluorine as compared to carbon leads to the 1s electrons being closer to the nucleus and results in greater diamagnetic shielding than is found with carbon.

(14) Gaussian 99, Development Version (Revision B.04): Frisch, M. J.; Trucks, G. W.; Schlegel, H. B.; Scuseria, G. E.; Robb, M. A.; Cheeseman, J. R.; Zakrzewski, V. G.; Montgomery, J. A., Jr.; Stratmann, R. E.; Burant, J. C.; Dapprich, S.; Millam, J. M.; Daniels, A. D.; Kudin, K. N.; Strain, M. C.; Farkas, O.; Tomasi, J.; Barone, V.; Cossi, M.; Cammi, R.; Mennucci, B.; Pomelli, C.; Adamo, C.; Clifford, S.; Ochterski, J.; Petersson, G. A.; Ayala, P. Y.; Cui, Q.; Morokuma, K.; Malick, D. K.; Rabuck, A. D.; Raghavachari, K.; Foresman, J. B.; Ortiz, J. V.; Baboul, A. G.; Cioslowski, J.; Stefanov, B. B.; Liu, G.; Liashenko, A.; Piskorz, P.; Komaromi, I.; Gomperts, R.; Martin, R. L.; Fox, D. J.; Keith, T.; Al-Laham, M. A.; Peng, C. Y.; Nanayakkara, A.; Challacombe, M.; Gill, P. M. W.; Johnson, B.; Chen, W.; Wong, M. W.; Andres, J. L.; Gonzalez, C.; Head-Gordon, M.; Replogle, E. S.; Pople, J. A. Gaussian, Inc., Pittsburgh, PA, 1998.

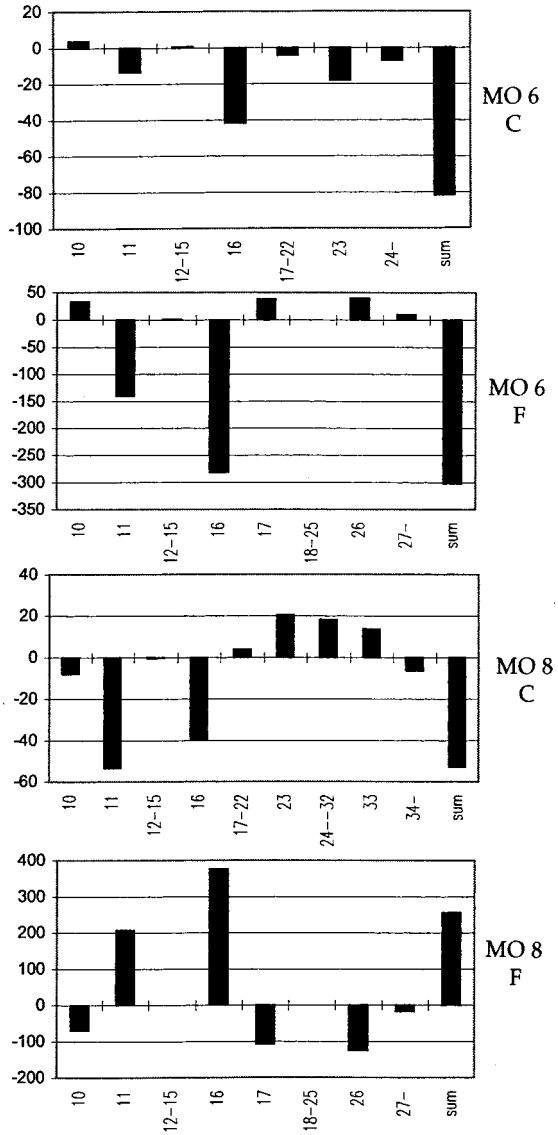

Figure 3. Coupling (ppm) between occupied MOs 6 and 8 and the virtual orbitals for methyl fluoride. The numbers of the latter are given below the plots.

The diamagnetic shielding does not change much with environment, and so, most of the difference in shielding for ^{19}F and ^{13}C results from the paramagnetic terms.

3. Isotropic Shielding

The calculated isotropic shielding for both ^{19}F and ^{13}C for the compounds in this report are given in Table 1 along with the observed shielding values. It can be seen that there is good agreement between experiment and theory. However, these data by themselves do not provide an insight into the reasons for the large changes in shielding. The shieldings for CH_3Cl to CCl_4 were calculated to serve as a comparison for the CH_3F to CF_4 series. One would not expect the calculations for the chlorides to be as successful as for the fluorides since they neglect spin−orbit coupling, which begins to become important for the second-row elements.[15] It can be seen that the changes in shielding for the two series are in the same direction, indicating that they are not due to some special property of the fluorines.

(15) Ballard, C. C.; Hada, M.; Kaneko, H.; Nakatsuji, H. *Chem. Phys. Lett.* **1996**, *254*, 170.

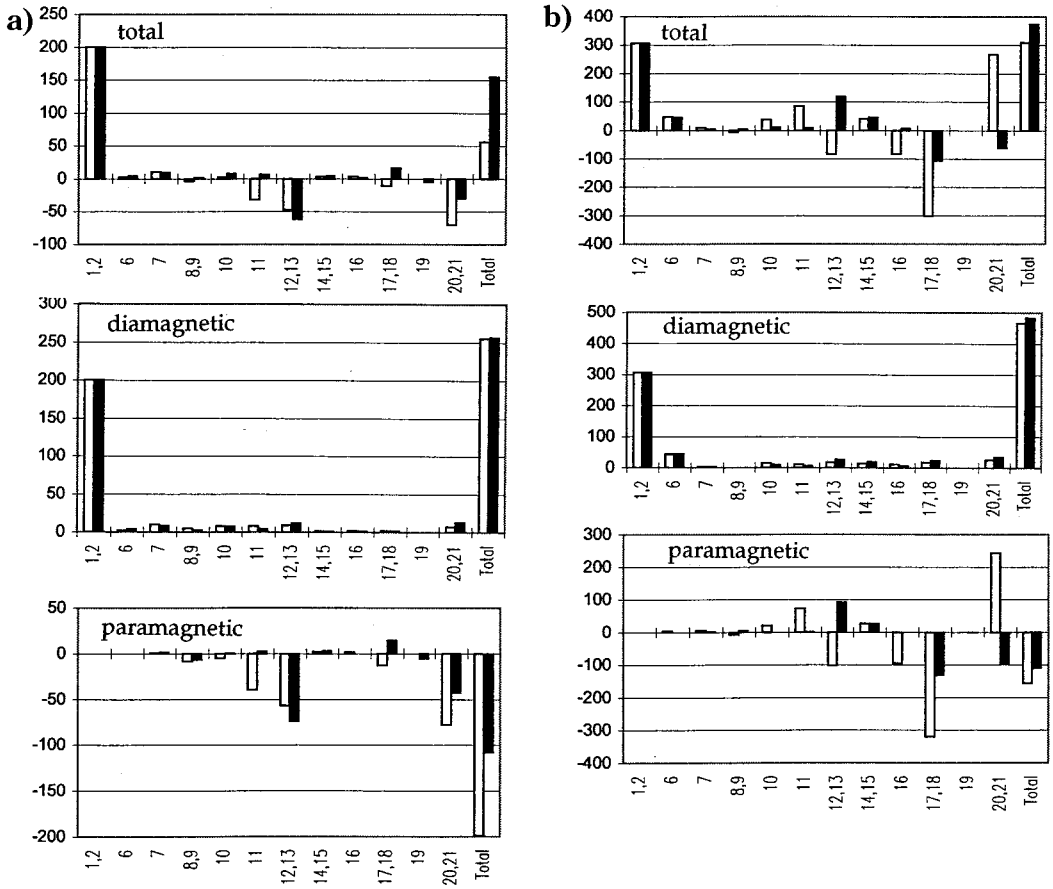

Figure 4. Magnetic shielding for *tert*-butyl fluoride on an MO basis. (a) Carbon: the upper plot gives the total shielding, the center plot gives the diamagnetic shielding, and the lower plot gives the paramagnetic shielding. (b) Fluorine: the ⊥ components are indicated by open bars, and the || components are indicated by solid bars.

To gain further information, we shall make use of the tensor components of the shielding that lie along the three orthogonal axes at a given nucleus and when averaged give the isotropic shielding. We shall also separate the diamagnetic and paramagnetic terms. They are dependent on the choice of origin for the calculations, and we shall make use of the nuclear center as the origin for a given nucleus. In addition, we shall separate the shielding components $\sigma_\perp$ (= σ_x and σ_y) and $\sigma_\parallel$ (= σ_z) into contributions from each of the occupied MOs. With these additional data, it should be possible to determine the origin of the changes in shielding.

4. Alkyl Fluorides

There is a significant change in geometry on going from methyl fluoride to *tert*-butyl fluoride, with the former having a 109.1° calculated HCF bond angle and a 1.379 Å C−F bond length and the latter having a 106.5° CCF bond angle and a 1.413 Å C−F bond length (Table 2). The smaller than tetrahedral angle is due to the high electronegativity of fluorine, which leads to higher p-character in the bond from carbon to fluorine (Bent's rule[16]). The difference between the HCF bond angle in methyl fluoride and the CCF bond angle in *tert*-butyl fluoride is probably due to the steric interaction among the three methyl groups of *tert*-butyl fluoride, and this change in angle would lead to a change in hybridization and an increase in the C−F bond length.

Is it possible that the changes in shielding are due to the changes in hybridization? This is explored in Table 3, which gives the effect of changing the HCF bond angle of methyl fluoride on the shielding at carbon and fluorine. It can be seen that the effect on the fluorine shielding is negligible and that only a part of the effect at carbon can be attributed to the geometry change. It might also be noted that the AIM[17] calculated charges at fluorine are essentially the same for this group of compounds.[18] Therefore, the changes in shielding cannot be attributed to changes in electron density at fluorine.

The tensor components at the fluorines of these compounds are summarized in Table 4. In each case, the C−F bond was aligned with the *z*-axis, and the *xz* plane was the symmetry plane. It can be seen that σ_z changes somewhat on going from methyl fluoride to ethyl fluoride but then remains essentially constant. On the other hand, the σ_x and σ_y tensor components change steadily on going through the series of halides. It might be noted that the anisotropy of the shielding for methyl fluoride has been determined experimentally and is 66 ± 8 ppm.[19] Our calculated value, 66 ppm, is in excellent agreement with the experiments.

(16) Bent, H. *Chem. Rev.* **1961**, *61*, 275.

(17) Bader, R. F. W. *Atoms in Molecules, A Quantum Theory*; Clarendon Press: Oxford, 1990.

(18) The calculated charges at fluorine for methyl fluoride, ethyl fluoride, isopropyl fluoride, and *tert*-butyl fluoride are −0.659, −0.662, −0.663, and −0.662, respectively. They were calculated using AIMALL, unpublished computer code by, T. A.Keith, based on PROAIM (Biegler-König, F. W.; Bader, R. F. W.; Tang, T.-H. *J. Comput. Chem.* **1982**,*3*, 317).

(19) Hunt, E.; Meyer, H. *J. Chem. Phys.* **1964**, *41*, 353.

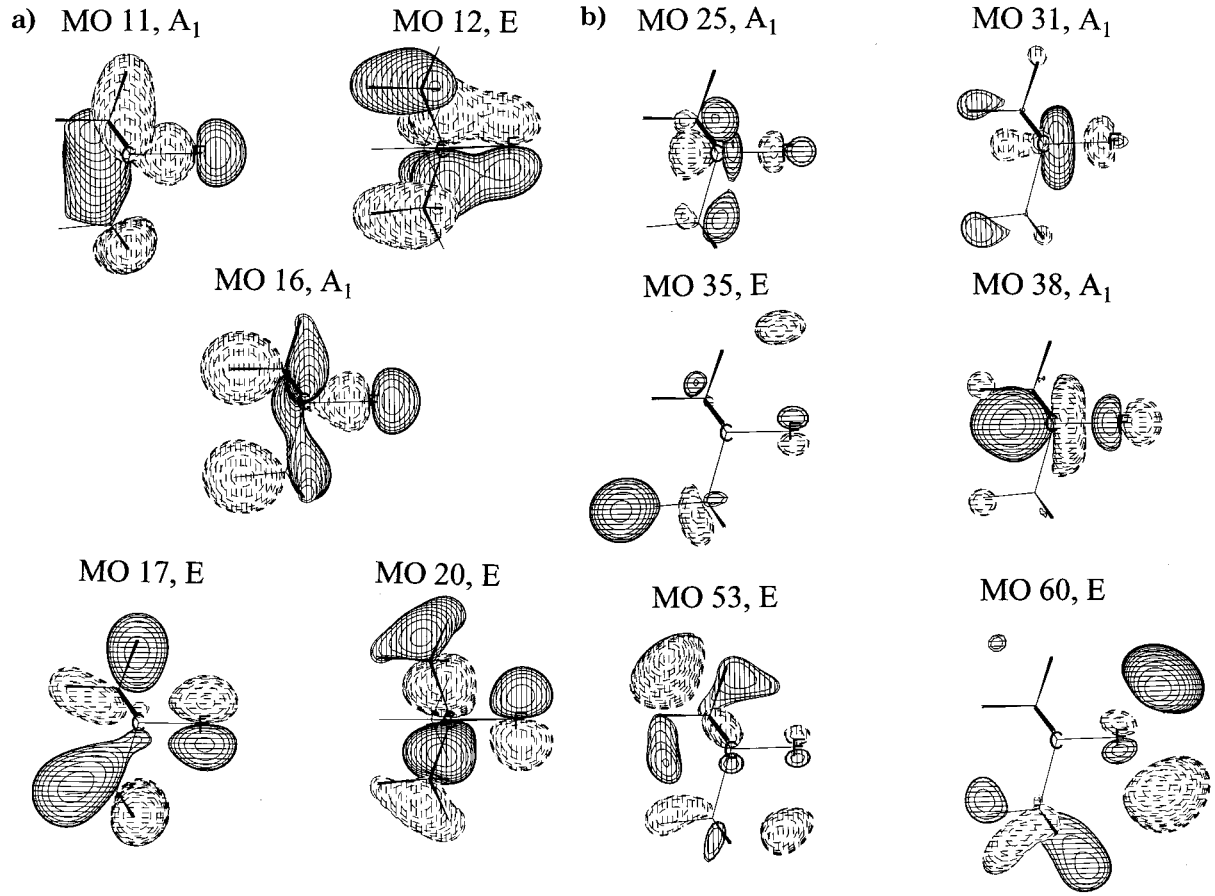

Figure 5. Molecular orbitals of *tert*-butyl fluoride: (a) occupied orbitals; (b) virtual orbitals.

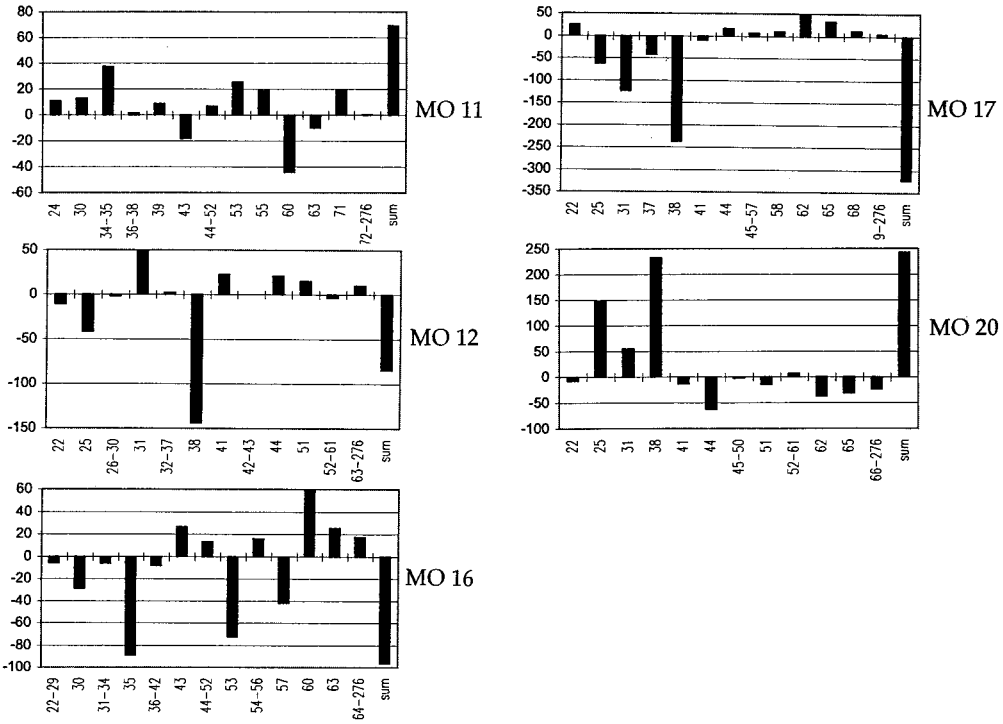

Figure 6. Coupling (ppm) between occupied MOs 11, 12, 16, 17, and 20 and the virtual orbitals for the F of *tert*-butyl fluoride. The numbers of the latter are given below the plots.

To obtain further information, the diamagnetic and paramagnetic terms were calculated on an MO basis giving Figure 1 for methyl fluoride and Figure 4 for *tert*-butyl fluoride. In these Figures, the ⊥ components of the shielding are indicated by open bars and the || components are indicated by solid bars. We have presented

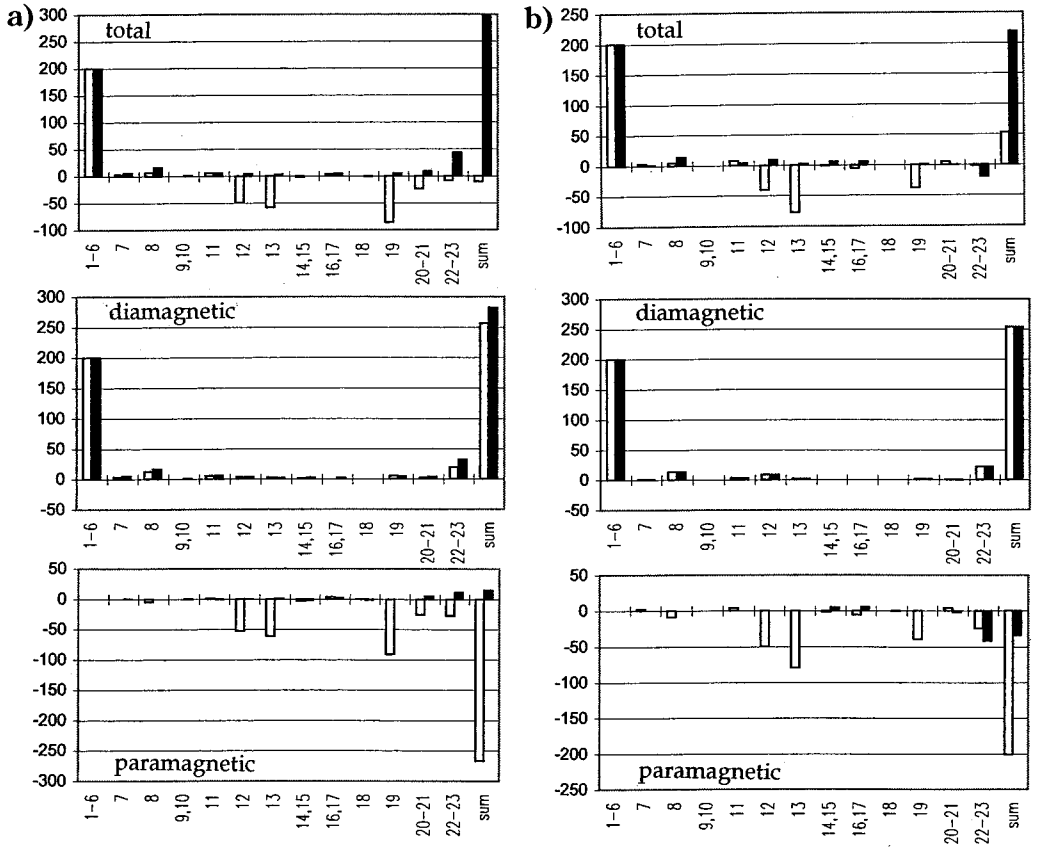

Figure 7. Magnetic shielding for *tert*-butylacetylene on an MO basis. (a) Cα: the upper plot gives the total shielding, the center plot gives the diamagnetic shielding and the lower plot gives the paramagnetic shielding. (b) Cβ: the ⊥ components are indicated by open bars, and the || components are indicated by solid bars.

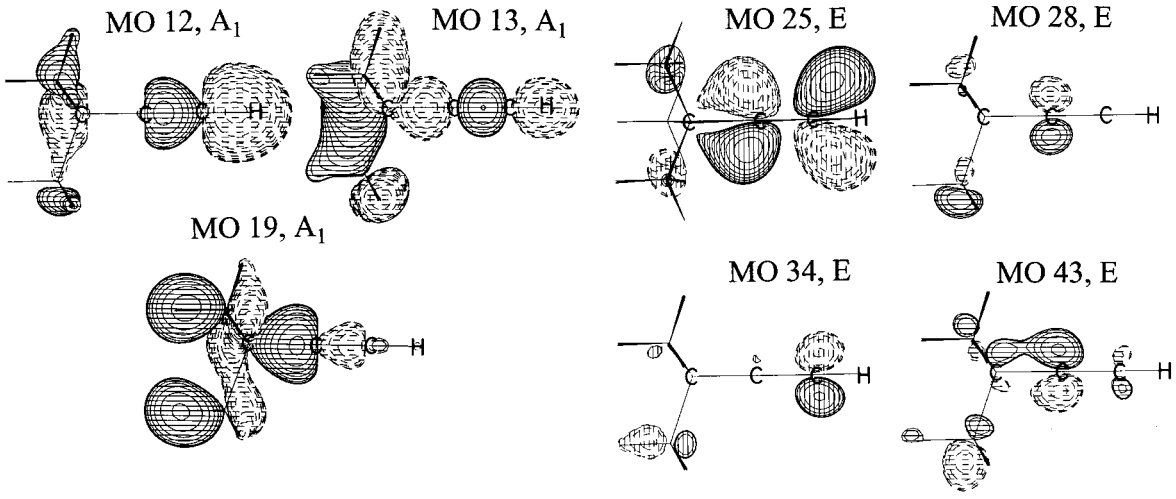

Figure 8. Molecular orbitals of *tert*-butylacetylene. MOs 12, 13, and 19 are occupied; the others are virtual orbitals.

Table 5. NMR Shielding (ppm) for the Carbons of Acetylenes

	Cα				Cβ			
compd	$\sigma_{x,y}$	σ_z	σ_{iso}	obsd	$\sigma_{x,y}$	σ_z	σ_{iso}	obsd
acetylene	29	279	112	115	29	279	112	115
methylacetylene	8	293	103	102	42	261	115	114
tert-butylacetylene	−11	298	92		54	247	118	

these data for methyl fluoride previously,[8] but they are repeated here to facilitate a comparison with *tert*-butyl fluoride. These compounds represent the extremes of the shielding values in this series, and the C_{3v} symmetry eliminates cross-terms at fluorine and the carbon attached to it. The $\sigma^{P}_{\perp}$ term for the fluorine of methyl fluoride is quite small, mainly because the effect of the degenerate π MOs 6 and 7 is essentially canceled by the degenerate π' MOs 8 and 9. These MOs are shown in Figure 2, and both interact with the σ^* MOs 11 and 16 in the presence of a magnetic field (Figure 3). The phase of the two p-atomic orbitals in 6 and 7 is the same, and when rotated 90° by the angular momentum operator, they match the phase of the p-orbitals in the σ^* MOs. As a result, they will give a deshielding paramagnetic interaction at both C and F. However, the phase of the

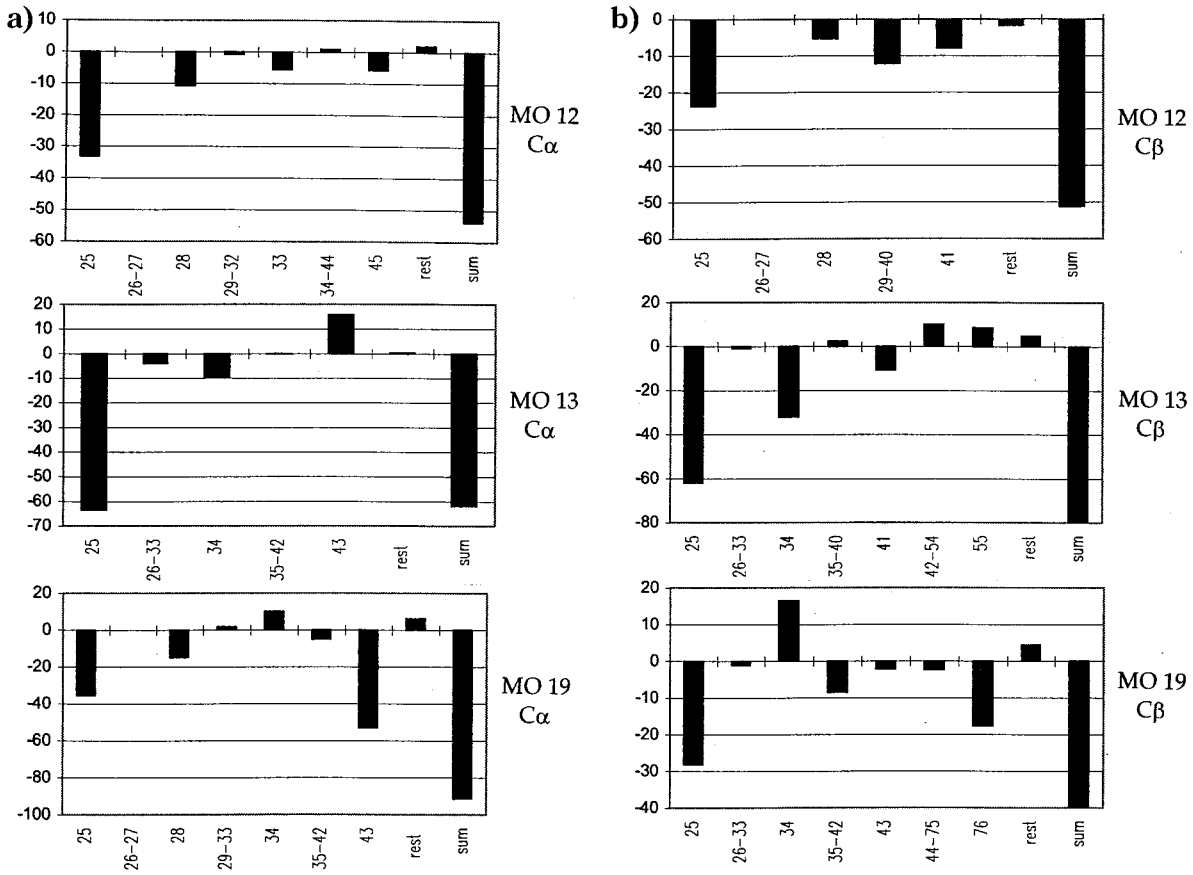

Figure 9. Coupling (ppm) between occupied MOs 12, 13, and 19 and the virtual orbitals of *tert*-butylacetylene: (a) C_α; (b) C_β.

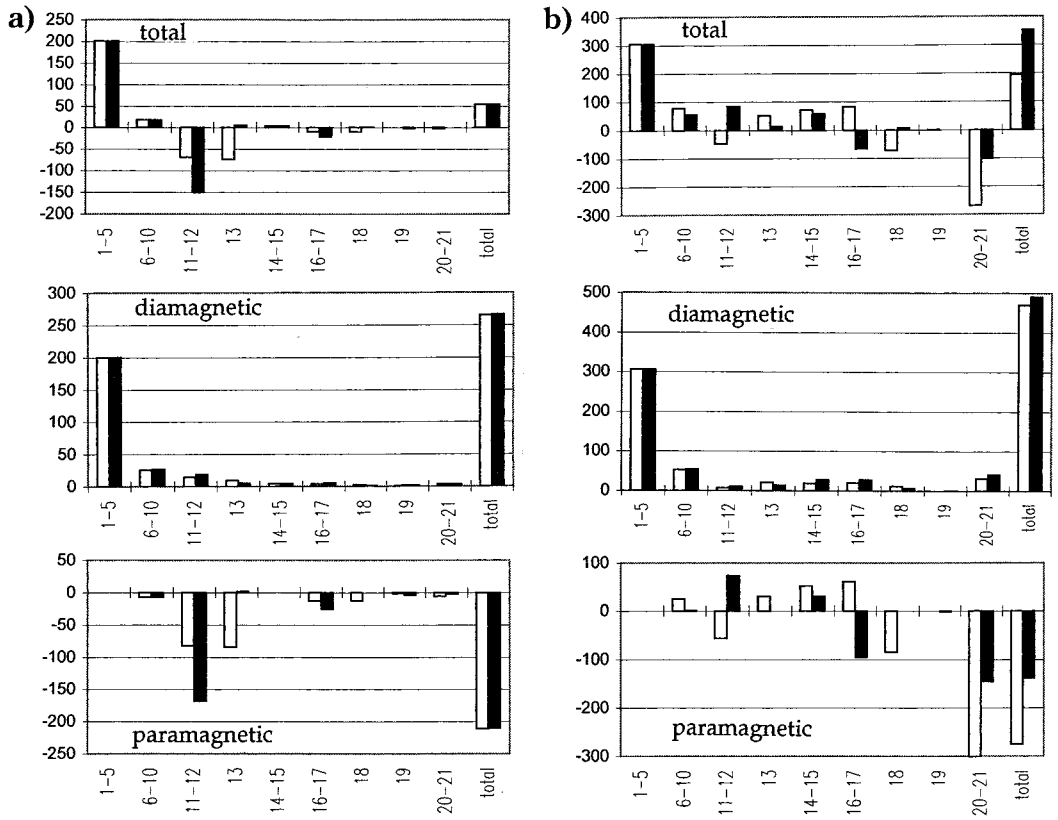

Figure 10. Magnetic shielding for carbon tetrafluoride on an MO basis. (a) Carbon: the upper plot gives the total shielding, the center plot gives the diamagnetic shielding, and the lower plot gives the paramagnetic shielding. (b) fluorine.

Table 6. NMR Shielding (ppm) for the Methyl Groups of Ethane and Neopentane

compd	σ_{xy}	σ_z	σ_{iso}	σ_{obs}
ethane	173	186	177	180
neopentane	139	186	154	159

AOs in MOs 8 and 9 is opposite, and when rotated by the angular momentum operator, their phase does not match that in σ^* MOs. This leads to a deshielding paramagnetic term at carbon and a shielding term at fluorine.[8]

MOs 17 and 18 of *tert*-butyl fluoride correspond to MOs 6 and 7 of methyl fluoride, and MOs 20 and 21 of *tert*-butyl fluoride correspond to MOs 8 and 9 of methyl fluoride (Figure 5). A comparison of Figures 1 and 4 shows that *x* or *y* axis paramagnetic terms for these pairs of orbitals are essentially the same for the two molecules and come close to canceling each other. Therefore, the increased $\sigma_\perp$ paramagnetic deshielding for *tert*-butyl fluoride results from the degenerate MOs 12 and 13 and MO 16. MOs 12 and 13 again involve a p-orbital at fluorine having a bonding interaction with the methyl group orbitals, and they couple mainly with the σ^* virtual orbital 38 to give paramagnetic deshielding (Figure 6). The σ MO 16 couples with the π^* MOs 35, 53, and 57, again leading to paramagnetic deshielding.

It seems clear that the decrease in $\sigma_\perp$ (increase in paramagnetic terms) in the series from methyl fluoride to *tert*-butyl fluoride results simply from having more p-AOs that can couple with the fluorine in forming the occupied MOs. The interaction of these MOs with the virtual MOs leads to the increased paramagnetic deshielding.

If this interpretation is correct, similar effects should be seen in other systems where methyl groups are replaced by *tert*-butyl. One possible example would be monosubstituted acetylenes. Table 5 gives the results of calculations for acetylene, methylacetylene, and *tert*-butylacetylene.

At C_α (the one bearing the substituent), the shielding about the *x* and *y* axes decreases with increasing alkyl substitution, just as found with the alkyl fluorides. At the same time, the shielding about the *z* axis increases. The effects at C_β are just the opposite. The contribution of each of the MOs to the paramagnetic terms was calculated and is shown in Figure 7. It can be seen that the principal contributions arise from MOs 12, 13, and 19 (Figure 8). The interaction of these MOs with the virtual MOs is shown in Figure 9. The main interaction terms arise from MOs 25, 28, 34, and 43 (Figure 8).

With acetylene, the *x* and *y* paramagnetic terms arise mainly from the interaction of the occupied σ orbital with a π^* orbital in the presence of a magnetic field. MO 13 of *tert*-butylacetylene corresponds to the acetylene σ orbital and MO 25 corresponds to the lower energy σ^* acetylene MO. But, in contrast to acetylene, the *tert*-butyl derivative has two other occupied σ orbitals (MOs 12 and 19). All three of these σ orbitals interact with MO 25 in the presence of a magnetic field to give substantial paramagnetic deshielding (Figure 9).

The main difference in the paramagnetic terms for C_α and C_β arises from MO 19, which leads to −92 ppm at C_α and −40 ppm at C_β. MO 19 gives a large coupling term at C_α with MO 43, whereas it is very small at C_β. It can be seen that MO 43 has a large p AO component at C_α, but only a small one at C_β, which can account for the difference.

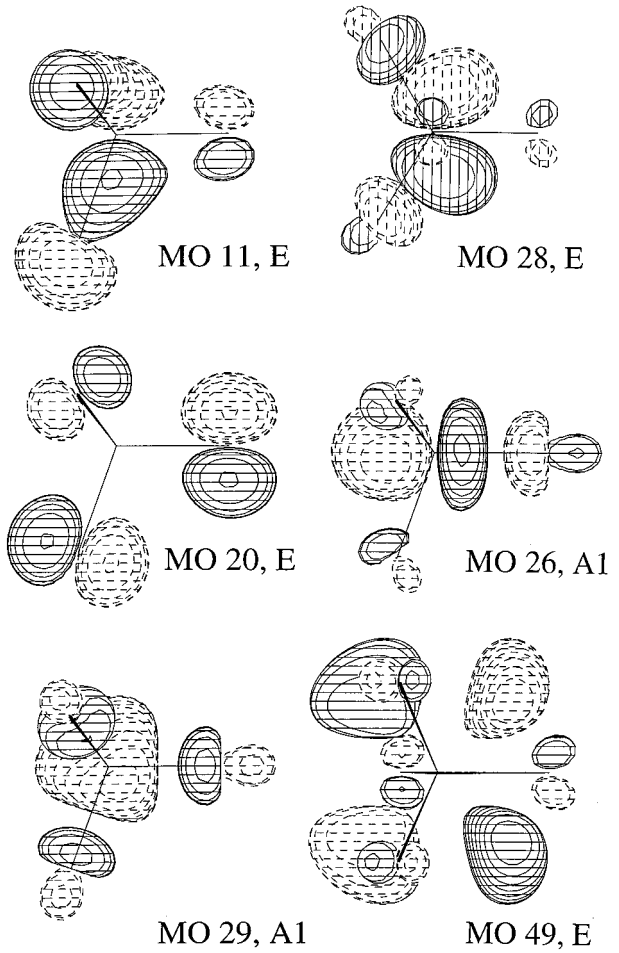

Figure 11. Molecular orbitals of carbon tetrafluoride. MOs 11 and 20 are occupied. Note that MOs 28 and 49 are rotated 90° about the *z* axis.

The same trend is found with such simple compounds as ethane and neopentane. The methyl group in neopentane is less shielded than that in ethane by 40 ppm. The calculated tensor components of the shielding are given in Table 6. Whereas the tensor component about the $C-CH_3$ axis is the same for the two compounds, the components perpendicular to this axis differ by 34 ppm. This is the same effect that was seen with the alkyl fluorides and the alkyl-substituted acetylenes, and presumably has the same origin.

5. Fluorinated Methanes

Carbon tetrafluoride has triply degenerate orbitals, which makes it difficult to compare it with methyl fluoride. Therefore, the symmetry was reduced by stretching one of the CF bonds by 0.0001 Å. This did not lead to a significant change in energy, but reduced the symmetry to C_{3v}, and makes it possible to concentrate on one fluorine that lies on the *z* axis. The shielding components on an MO basis are shown in Figure 10.

The $\sigma_\perp$ and $\sigma_\parallel$ tensor components of the shielding have been derived from low-temperature NMR measurements on clathrates and are 213 ± 14 and 352 ± 15 ppm,

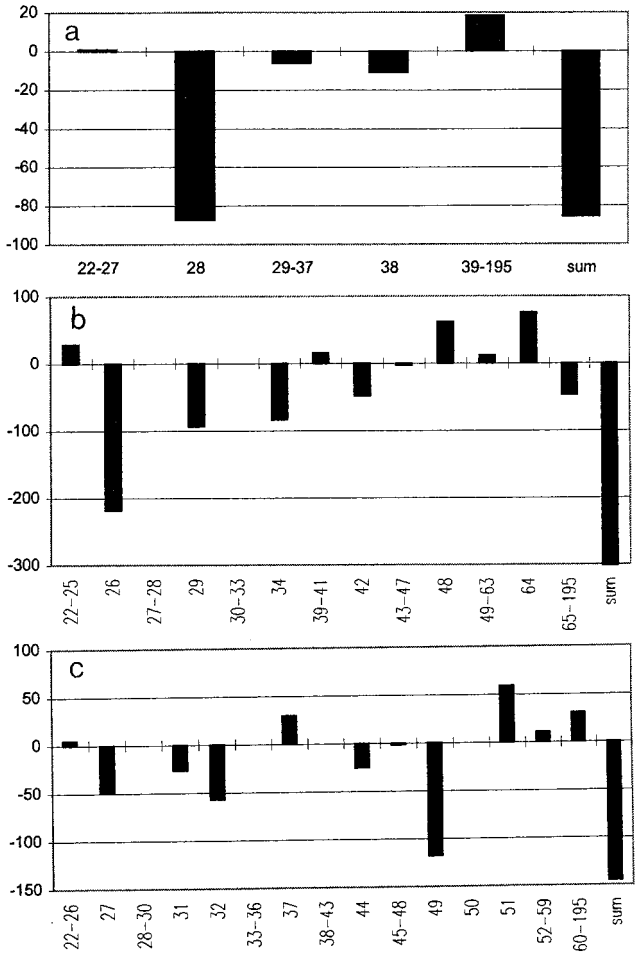

Figure 12. Coupling (ppm) between occupied and virtual orbitals for carbon tetrafluoride: (a) ^{13}C, MO 11; (b) ^{19}F, MO 20, *xy*; (c) ^{19}F, MO 20, *z*.

respectively.[20] The calculated values, 193 and 352 ppm, are in good agreement with the experiments.

A comparison of Figures 1 and 4 shows that the fluorine of CF_4 is quite different than that in the fluoroalkanes. Here, there are several occupied MOs that give small paramagnetic shielding and deshielding terms that average to essentially zero. The paramagnetic terms derived from MOs 20 and 21 are essentially equal to the total of the paramagnetic terms.

This pair of degenerate MOs have essentially pure p-functions at the carbons (Figure 11). The lack of mixing with the other atomic functions is probably the cause of the strong coupling to the virtual orbitals. With a magnetic field applied along the *x* or *y* directions (perpendicular to the C−F bond in question), they will couple (cf. Figure 12) with A_1 MOs that have their fluorine p-orbital lying along the *z* axis, such as MOs 26 and 29 (Figure 11). With a magnetic field along the *z* direction, they will couple with the component of a degenerate pair (E) of MOs that lie along the *y* or *x* directions, respectively. In the case of MO 20, two appropriate MOs are 27 and 49. The larger paramagnetic contribution from MO 49 as compared to MO 27 is due to the larger p_y term for the former.

The shielding at the carbon of CF_4 is dominated by MOs 11, 12, and 13, which would be triply degenerate in the fully tetrahedral geometry. MO 11 couples with MO 28, which has its p-orbital at carbon rotated 90° with respect to that in MO 11. Similar interactions are found with the other members of this group, leading to a large paramagnetic term, and only a small total shielding value.

Summary

The ^{19}F shielding in a series of aliphatic fluorides has been accurately computed using the IGAIM method. Separating the shielding into tensorial components, and further classifying the shielding terms by the originating occupied orbitals, makes it possible to identify the factors that lead to the experimentally observed shielding trends. In these fluorides, there are large paramagnetic terms due to the presence of essentially pure p-orbitals on the fluorine atoms. Their net effect on the shielding depends on how these paramagnetic terms decompose into the usual type versus those of the Cornwall type. The latter arise when the relative phases of the atomic p-orbitals included in the molecular orbital are switched, leading to a paramagnetic term on the fluorine which is actually diamagnetic in its effect. Increasing substitution by fluorine leads to additional deshielding which is simply due to the increased participation of the fluorine p-orbitals in the molecular orbitals. This is a rather general substituent effect; whenever a give substituent is replaced by one with more p-character, increased paramagnetic deshielding is observed. Thus, the substitution of H by CH_3 leads to analogous increases in paramagnetic deshielding. The substituent effects on shielding by fluorine substitution are simply more pronounced as the orbitals introduced has such high p-character.

Acknowledgment is made to the donors of the Petroleum Research Fund, administered by the American Chemical Society, for support of this work. We thank Dr. James Cheeseman for his assistance in modifying Gaussian-99 to print the individual MO components of the shielding.

JO001726G

(20) Garg, S. K.; Ripmeester, J. P.; Davidson, D. W. *J. Chem. Phys.* **1982**, *77*, 2847.